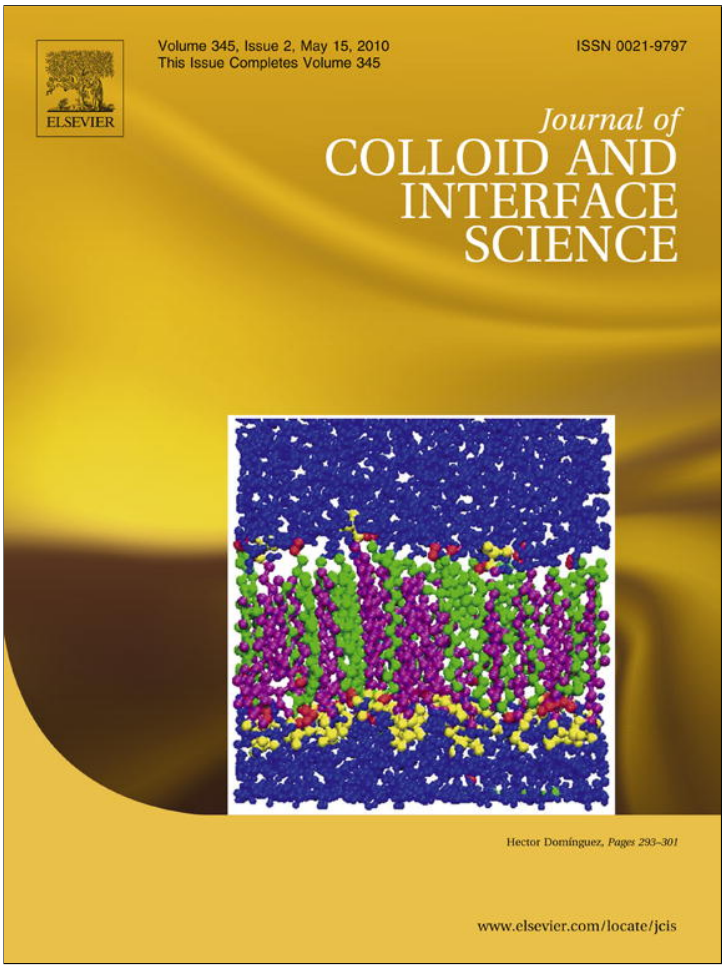

Journal of Colloid and Interface Science 345 (2010) 505–514

Contents lists available at ScienceDirect

Journal of Colloid and Interface Science

www.elsevier.com/locate/jcis

Interaction between like-charged particles at a liquid interface: Electrostatic repulsion vs. electrocapillary attraction

Krassimir D. Danov, Peter A. Kralchevsky *

Department of Chemical Engineering, Faculty of Chemistry, Sofia University, 1164 Sofia, Bulgaria

ARTICLE INFO

Article history:
Received 6 January 2010
Accepted 9 February 2010
Available online 13 February 2010

Keywords:
Particles at a liquid interface
Electrocapillary attraction
Electrodipping force

ABSTRACT

The electric field of charged particles, which are adsorbed at a liquid interface, induces interfacial deformations (capillary menisci). The overlap of such deformations gives rise to electrocapillary force of interaction between the particles. Our goal is to quantify this interaction on the basis of a force approach, which is different from the approaches (mostly based on energy calculations) used by other authors. The fact that the electric field of adsorbed particles has a dipolar asymptotics (due to the image-charge effect) is utilized to derive an analytical expression for the meniscus profile. The comparison of the calculated profile with experimental data indicates that the results based on the dipolar approximation agree excellently with the data, except some small deviations near the contact line. The effect of the interfacial deformation on the electrostatic pressure is also taken into account. The two-particle electrocapillary problem is solved in bipolar coordinates without using the superposition approximation. It turns out that for uniform distribution of the surface charges, the electrocapillary attraction is weaker than the electrostatic repulsion at interparticle distances at which the dipolar approximation is applicable, so that the net force is repulsive. This result is in agreement with the conclusions of other authors obtained by using different theoretical approaches and with available experimental data. The analytical expressions for the electrocapillary and electrodipping forces derived in the present article provide a simple and convenient way for estimation of these forces.

1. Introduction

The electric field of charged particles that are adsorbed at a liquid interface induces interfacial deformations, which lead to lateral capillary interactions [1]. Lateral capillary forces have been investigated during the last 15 years in relation to their importance for creation of two-dimensional structures of colloids (including protein molecules and nanoparticles) with various applications [2–14]. Comprehensive reviews can be found in Refs. [15–23].

In the case of charged particles, the electric field acts simultaneously on the particles and on the surrounding liquid interface. For this reason, the capillary meniscus around a given adsorbed particle decays $\propto 1/r^4$ (rather than logarithmically) with the increase of the radial distance r to the particle [24]. (For noncharged particles, the meniscus has logarithmic asymptotics, which is related to the asymptotic behavior of the modified Bessel function $K_0(x)$ at small x; see e.g. Refs. [16,18].) The existence of electrodipping force, F_{ED}, that pushes a charged particle toward the phase of greater dielectric constant was experimentally proven with particles at air/water and oil/water interfaces, and theory for the calculation of this force was developed [25,26]. The meniscus shape around individual charged particles was experimentally determined and the results were compared with the theoretical predictions [27].

The two-particle problem was addressed by Foret and Würger [28], who concluded that the force of direct electric repulsion between two like-charged particles and the force of electrocapillary attraction between them have similar asymptotic behavior at large distances: $|F_{ER}| \propto |F_{EC}| \propto 1/L^4$, where L is the interparticle distance [29]; see Fig. 1. It was still unclear whether the attraction, F_{EC}, can prevail over the repulsion, F_{ER} [29]. Oettel et al. [30] confirmed that the meniscus shape cannot have logarithmic shape unless the particles experience the action of some additional external force. These authors independently established that the asymptotics of the electrocapillary force is $F_{EC} \propto 1/L^4$ [31], and arrived at the conclusion that at asymptotically large separations the capillary attraction does not overcome the direct electrostatic repulsion between the colloidal particles [32]. This conclusion was confirmed in experiments with micrometer-sized polystyrene particles using laser tweezers [33].

Attraction between like-charged particles of radii 200—300 μm floating at an oil/water interface was experimentally detected on the background of the gravity-induced lateral capillary force [34]. This attraction was interpreted as a hybrid capillary interaction between a gravity-induced capillary charge and a capillary

* Corresponding author. Fax: +359 2 962 5643.
E-mail address: pk@lcpe.uni-sofia.bg (P.A. Kralchevsky).

0021-9797/$ - see front matter © 2010 Elsevier Inc. All rights reserved.
doi:10.1016/j.jcis.2010.02.017

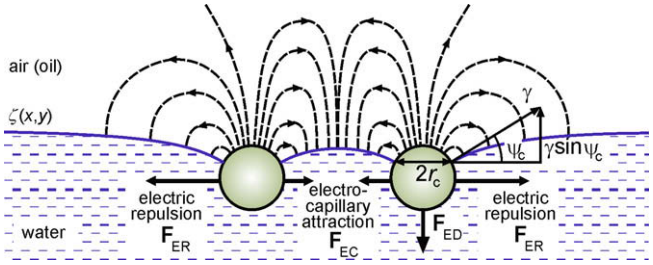

Fig. 1. Sketch of two like-charged particles attached to an oil–water interface. F_{ED} is the electrodipping force, due to the image-charge effect, that pushes the particles into water and deforms the fluid interface around them; F_{ER} is the direct electric repulsion between the particles; F_{EC} is the electrocapillary attraction, related to deformations in the fluid interface created by the electric field; ψ_c is the meniscus slope angle at the contact line of radius r_c; γ is the interfacial tension.

quadrupole induced by anisotropically distributed surface charges on the particle/oil interface [35].

A particle with uniformly distributed surface charges, which is adsorbed at a water/nonpolar-fluid interface, creates electric field that has asymptotically dipolar character. The force of electrostatic repulsion between two such particles – parallel dipoles is [36–41]:

$$F_{ER} = \frac{3p_d^2}{2\varepsilon_n L^4}(L \gg r_c, \kappa^{-1}), \tag{1.1}$$

where L is the center-to-center distance between the two particles; r_c is the radius of their contact lines; ε_n is the dielectric constant of the nonpolar fluid (air, oil); p_d is an effective dipole moment. The factor 2 in the denominator of Eq. (1.1) accounts for the fact that the dipolar field occupies only the upper half-space (the nonpolar fluid), whereas the electric field in the aqueous phase is screened by the ions in water. The electric charges that create the electric field can be located at the particle/water interface [22,29,36–38] and/or on the particle/nonpolar-fluid interface [9,10,25–27,34,35,39–43]. Eq. (1.1) is applicable in both cases, as follows.

If the charges are located at the *particle/nonpolar-fluid* interface, then the effective dipole moment p_d is given by the expression [26]:

$$p_d = 4\pi\sigma_{pn} D R^3 \sin^3\alpha. \tag{1.2}$$

Here, R is the particle radius, α is a central angle ($\sin\alpha = r_c/R$), and σ_{pn} is the electric charge density at the particle/nonpolar-fluid interface; $D = D(\alpha, \varepsilon_{pn})$ is a known dimensionless function, which can be calculated by means of Table 1 and Eq. (D.1) in Ref. [26]; $\varepsilon_{pn} \equiv \varepsilon_p/\varepsilon_n$ is the ratio of the dielectric constants of the particle and nonpolar fluid.

If charges are located at the *particle/water* interface, then the effective dipole moment p_d can be estimated from the expression [22,33,37,38]:

$$p_d = \frac{2\varepsilon_n q}{\varepsilon_w \kappa}, \tag{1.3}$$

where ε_w is the dielectric constant of water; q is the total surface charge, and κ is the Debye screening parameter.

Here, our goal is to directly calculate the force of electrocapillary interaction between two like-charged particles located at a water/nonpolar-fluid interface. The approach used in Ref. [35] is further developed and applied to the case of isotropic charge distribution on the particle surface. The interaction force is calculated by integrating the interfacial tension along the particle contact line and the pressure tensor over the particle surface. The effect of the meniscus shape on the electric field is taken into account by means of a four-step iteration procedure (Section 2). The meniscus profile around a pair of adsorbed particles is determined by solving the Young–Laplace equation in bipolar coordinates, without using the capillary superposition approximation (Section 3). The total interaction force is obtained in the form of a series in powers of r_c/L, and the contributions of the direct electric repulsion and electrocapillary attraction are compared (Section 4).

It should be noted that at short distances between small particles of radius comparable to the Debye length, κ^{-1}, the direct electric repulsion includes a screened coulomb term besides the dipole term [37,38,44]. In the present study we consider particles of size much greater than κ^{-1}, for which the dipole term is predominant; see e.g. the experimental system in Ref. [33] and that in Section 3.2 below.

2. Basic equations

Let us consider two electrically charged particles, like those in Fig. 1, which are located at the boundary between water and a nonpolar fluid (air or oil). The charged particles create electric field, which gives rise to mechanical stresses described by the Maxwell pressure tensor [45]:

$$\mathbf{P}_w = \left(p_w + \frac{\varepsilon_w}{8\pi}\nabla\varphi_w\cdot\nabla\varphi_w\right)\mathbf{U} - \frac{\varepsilon_w}{4\pi}\nabla\varphi_w\nabla\varphi_w, \tag{2.1}$$

$$\mathbf{P}_n = \left(p_n + \frac{\varepsilon_n}{8\pi}\nabla\varphi_n\cdot\nabla\varphi_n\right)\mathbf{U} - \frac{\varepsilon_n}{4\pi}\nabla\varphi_n\nabla\varphi_n, \tag{2.2}$$

where the subscripts "w" and "n" denote quantities related, respectively, to the water and nonpolar-fluid phases; $\mathbf{U}$ is the spatial unit tensor; p_w and p_n are the scalar (hydrostatic) pressures in the respective phases, whereas φ_w and φ_n are the electrostatic potentials in these phases.

At equilibrium, the shape of the liquid interface obeys the Young–Laplace equation [46]:

$$2H\gamma = \mathbf{n}_s\cdot(\mathbf{P}_n - \mathbf{P}_w)\cdot\mathbf{n}_s \quad \text{at } z = \zeta, \tag{2.3}$$

where H is the mean curvature of the liquid surface $z = \zeta(x,y)$; $\mathbf{n}_s$ is its running unit normal directed toward the nonpolar-fluid phase; γ is the respective interfacial tension. The substitution of Eqs. (2.1) and (2.2) into the right-hand-side of Eq. (2.3), yields:

$$2H\gamma = p_n + \frac{\varepsilon_n}{8\pi}[(\mathbf{n}_s\times\nabla\varphi_n)^2 - (\mathbf{n}_s\cdot\nabla\varphi_n)^2] - p_w - \frac{\varepsilon_w}{8\pi}[(\mathbf{n}_s\times\nabla\varphi_w)^2 - (\mathbf{n}_s\cdot\nabla\varphi_w)^2] \quad \text{at } z = \zeta, \tag{2.4}$$

where we have used the vectorial identity $\mathbf{A}^2\mathbf{B}^2 = (\mathbf{A}\times\mathbf{B})^2 + (\mathbf{A}\cdot\mathbf{B})^2$ with $\mathbf{A} = \mathbf{n}_s$ and $\mathbf{B} = \nabla\varphi$.

The force acting on an adsorbed particle is [47]:

$$\mathbf{F} = \mathbf{F}^{(p)} + \mathbf{F}^{(\gamma)}, \tag{2.5}$$

where the $\mathbf{F}^{(p)}$ represents the integral of pressure tensor over the particle surface, S, and $\mathbf{F}^{(\gamma)}$ is the integral of the interfacial tension (considered as a vector) over the contact line C:

$$\mathbf{F}^{(p)} = -\int_{S_w} d\mathbf{S}\cdot\mathbf{P}_w - \int_{S_n} d\mathbf{S}\cdot\mathbf{P}_n, \quad \mathbf{F}^{(\gamma)} = \int_C dl\mathbf{m}\gamma. \tag{2.6}$$

Here and hereafter, γ is the interfacial tension of the liquid interface (oil/water or air/water); see Fig. 1; S_w and S_n are the portions of the particle surface that contact with the water and nonpolar-fluid phases, respectively; $d\mathbf{S}$ is a vectorial surface element; dl is the scalar linear element of the contact line C; $\mathbf{m}$ is the outward pointing unit normal field having the direction of the surface tension at the contact line, i.e. normal to C and tangential to the liquid interface.

Here, we will consider particle sizes and interparticle distances that are much greater than the Debye screening length in the aqueous phase. The dielectric constant of water, ε_w, is supposed to be much greater than those of the particle, ε_p, and of the nonpolar fluid, ε_n: i.e. $\varepsilon_w \gg \varepsilon_p, \varepsilon_n$. For this reason, the electric field created

by charges, located at the *particle/nonpolar-fluid* interface, practically does not penetrate into the water phase; see, for example, the known problems for the image-charge effect [45,48] and for a hydrophobic particle near an oil–water interface [49]. Experimentally, the non-penetration of the field into water is manifested as independence of the configuration of the adsorbed particles on the electrolyte concentration in the aqueous phase [25,27,41]. Moreover, charges on the *particle/water* interface can also create a long-range electric field that penetrates in the nonpolar fluid trough the particle [36–38], whereas their electric field is suppressed in the aqueous phase by the Debye screening. Thus, in first approximation, the role of the aqueous phase is to keep the electric potential constant at the particle/water and water/nonpolar-fluid interfaces. In such a case, we can set $\varphi_w \equiv 0$, and

$$\varphi_n = 0 \quad \text{at } z = \zeta(x,y). \tag{2.7}$$

In other words, the interface $z = \zeta(x,y)$ is equipotential. Then, the vector $\nabla\varphi_n$ is directed along the normal $\mathbf{n}_s$. Setting $\varphi_w = 0$ and $\mathbf{n}_s \times \nabla\varphi_n = 0$ in Eq. (2.4), and using the assumption for small meniscus slope, we obtain:

$$\frac{\partial^2\zeta}{\partial x^2} + \frac{\partial^2\zeta}{\partial y^2} = -\frac{\varepsilon_n}{8\pi\gamma}\left(\frac{\partial\varphi_n}{\partial z}\right)^2 \quad \text{at } z = \zeta. \tag{2.8}$$

We have used the assumption for small meniscus slope, $\zeta_x^2 + \zeta_y^2 \ll 1$, which is fulfilled for sub-millimeter particles, as well as the fact that the liquid interface is flat far from the particles, and hence $p_n = p_w$. In this paper, we neglect the effect of the gravitational hydrostatic pressure. For sub-millimeter particles, the effects of the electric and gravitational on the meniscus shape have been found to be additive [27].

Eq. (2.8), along with the boundary condition, Eq. (2.7), allows us to calculate the deformation of the liquid interface created by the particles and their electric field, as well as the interparticle force. For this goal, we will apply the following *iteration procedure*:

(1) In zero-order approximation, the electrostatic potential of two particles-dipoles, $\varphi_0(\mathbf{r})$, is calculated assuming that the liquid interface is flat and equipotential, i.e. $\varphi_0|_{z=0} = 0$; see Eqs. (3.1) and (3.2) below.
(2) Next, substituting $\varphi_n = \varphi_0$ in the right-hand-side of Eq. (2.8), we find the meniscus shape, $z = \zeta(x,y)$, in first approximation. After that, we determine $\mathbf{F}^{(\gamma)}$, i.e. the surface tension contribution to the interaction force.
(3) To find the next correction term, we will seek φ_n in the form:

$$\varphi_n = \varphi_0(\mathbf{r}) + \varphi_1(\mathbf{r}), \tag{2.9}$$

where φ_1 accounts for the effect of the interfacial deformation on the electrostatic potential φ_n. Expanding in series the boundary condition, Eq. (2.7), we obtain $0 = \varphi_n(x,y,\zeta(x,y)) = \varphi_n(x,y,0) + (\partial\varphi_n/\partial z)_{z=0}\zeta + \cdots$ In view of Eq. (2.9), having in mind that $\varphi_0|_{z=0} = 0$ we obtain:

$$\varphi_1 = -\frac{\partial\varphi_0}{\partial z}\zeta \quad \text{at } z = 0. \tag{2.10}$$

Thus, φ_1 is solution of the equation $\nabla^2\varphi_1 = 0$ (no ions in the nonpolar fluid), which satisfies the boundary condition, Eq. (2.10).

(4) With $\varphi_n = \varphi_0(\mathbf{r}) + \varphi_1(\mathbf{r})$, we calculate the Maxwell pressure tensor, $\mathbf{P}$, and then by using Eq. (2.6) we determine $\mathbf{F}^{(p)}$ and the total interaction force, $F_x = F_x^{(\gamma)} + F_x^{(p)}$.

The next step in the iteration procedure is to substitute $\varphi_n = \varphi_0(\mathbf{r}) + \varphi_1(\mathbf{r})$ in the right-hand-side of Eq. (2.8) and to determine the next correction in the meniscus profile $\zeta(x,y)$. However, it turns out that the resulting correction term is of the order of the neglected terms in Eq. (2.8) for small meniscus slope, $\zeta_x^2 + \zeta_y^2 \ll 1$, and hence this correction term is negligible in the framework of the used level of accuracy. For this reason, we will stop the iterations after completing the fourth step.

3. Theoretical model

3.1. Meniscus shape

We consider two identical adsorbed particles, *A* and *B*, separated at a center-to-center distance *L*, with circular contact lines of radius r_c on their surfaces (Fig. 2). As mentioned above, an adsorbed charged particle creates electric field, which has asymptotically dipolar character; see Eq. (1.1). For this reason, in zero-order approximation we will assume that the electric field created by the two particles in the nonpolar fluid is equivalent to the superposition of the fields of two dipoles:

$$\varphi_0 = \varphi_{A,0} + \varphi_{B,0}, \tag{3.1}$$

$$\varphi_{A,0} = \frac{p_d}{\varepsilon_n}\frac{z}{(\rho_A^2 + z^2)^{3/2}}, \quad \varphi_{B,0} = \frac{p_d}{\varepsilon_n}\frac{z}{(\rho_B^2 + z^2)^{3/2}}, \tag{3.2}$$

where p_d is the dipole moment, see Eqs. (1.2) and (1.3); ρ_A and ρ_B are radial distances with respect to the centers of the particles *A* and *B* (Fig. 3). The meniscus shape $z = \zeta(x,y)$ will be determined as a solution of Eq. (2.8) substituting $\varphi_n = \varphi_0$ in first approximation.

First, we will determine the profiles $z = \zeta_A(x,y)$ and $z = \zeta_B(x,y)$ of the menisci around each of the two particles *in isolation*. For this goal, in the right-hand-side of Eq. (2.8) we substitute $\varphi_n = \varphi_{Y,0}$, $Y = A, B$, from Eq. (3.2), which leads to:

$$\frac{1}{\rho_Y}\frac{d}{d\rho_Y}\left(\rho_Y\frac{d\zeta_Y}{d\rho_Y}\right) = -\frac{p_d^2}{8\pi\gamma\varepsilon_n\rho_Y^6}, \quad Y = A, B. \tag{3.3}$$

The first integral of Eq. (3.3) is:

$$\frac{d\zeta_Y}{d\rho_Y} = \frac{p_d^2}{32\pi\gamma\varepsilon_n\rho_Y^5}, \quad Y = A, B. \tag{3.4}$$

Setting $\rho_Y = r_c$ in Eq. (3.4), we determine the meniscus slope at the contact line (Fig. 1):

$$\delta \equiv \tan\psi_c = \frac{p_d^2}{32\pi\gamma\varepsilon_n r_c^5}. \tag{3.5}$$

Insofar as the meniscus slope is small, δ is a small parameter. This fact will be used below. Having in mind that the electrodipping force, F_{ED}, acting on each particle is counterbalanced by the vertical component of the surface-tension force, $F_{ED} = 2\pi\gamma r_c \sin\psi_c$ (Fig. 1), from Eq. (3.5) we obtain:

$$F_{ED} = \frac{p_d^2}{16\varepsilon_n r_c^4} \tag{3.6}$$

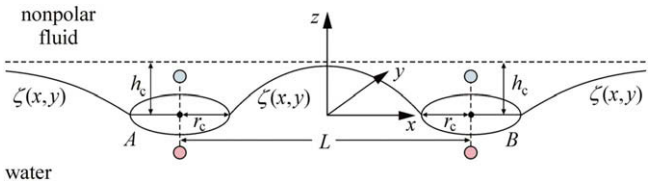

Fig. 2. Sketch of the meniscus profile, $z = \zeta(x,y)$, around two identical charged particles, *A* and *B*, which are attached to the boundary between a water phase and a nonpolar fluid (e.g. air or oil). The contact lines on the particle surfaces are presented by two circles of radius r_c. The distance between the plane of the contact lines and the plane of the non-perturbed liquid interface far from the particles is denoted by h_c. The dipoles associated with each particle in accordance with Eq. (3.2) are symbolically depicted.

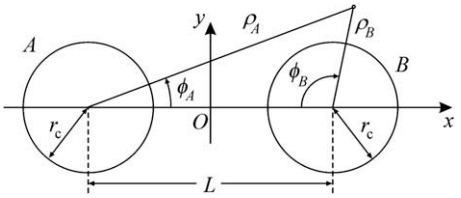

Fig. 3. Polar coordinates (ρ_A, ϕ_A) and (ρ_B, ϕ_B) in the xy-plane connected with two identical particles, A and B. The contact lines on the particle surfaces are circumferences of radius r_c; L is the distance between their centers.

($\sin\psi_c \approx \tan\psi_c$ at small meniscus slope). The integration of Eq. (3.4) yields the following expression for the meniscus shape around an isolated particle:

$$\zeta_Y = \frac{p_d^2}{128\pi\gamma\varepsilon_n}\left(\frac{1}{r_c^4} - \frac{1}{\rho_Y^4}\right), \quad Y = A, B. \tag{3.7}$$

The boundary condition $\zeta_Y(r_c) = 0$ has been used; see Fig. 2. As already mentioned, here we do not consider gravitational effects, so that $\zeta_Y(\rho_Y)$ is determined solely by the particle electric field. We have assumed that the xy-plane coincides with the plane of the particles' contact line, which is located at a distance h_c below the plane of the non-disturbed liquid interface far from the particles (Fig. 2). Setting $\rho_Y \to \infty$ in Eq. (3.7), we find:

$$h_c = \frac{p_d^2}{128\pi\gamma\varepsilon_n r_c^4}. \tag{3.8}$$

3.2. Discussion on the validity of the model

As mentioned above, in our model we consider particles of finite size, but their electric field is approximated with the field of dipoles, see Eq. (3.2). In general, this approximation is expected to become inaccurate close to the particle surface, where the electric field may deviate from the field of a dipole.

The model predicts that ζ_Y depends linearly on $1/\rho_Y^4$; see Eq. (3.7). In Fig. 4, we plot experimental data for the meniscus profile ζ_Y vs. $1/\rho_Y^4$. The data are from Ref. [27] and are obtained for a hydrophobized glass sphere of radius $R = 240.6$ μm located at the boundary water/tetradecane at contact-line radius $r_c = 236.1$ μm. For such a relatively large particle there is also gravitational deformation of the meniscus. The latter is calculated from available accurate theoretical expressions and subtracted from the total deformation [27] to obtain the purely electrostatic deformation $\zeta_Y(\rho_Y)$, which is plotted in Fig. 4. As seen in the figure, the plot of ζ_Y vs. $(r_c/\rho_Y)^4$ complies very well with a straight line except the closest vicinity of the contact line (at $0.96 < r_c/\rho_Y < 1$), where small deviations from the linear dependence are observed. This result indicates that the used approximation for dipolar electric field, Eq. (3.2), works very well and predicts the meniscus shape except some small deviations near the particle contact line.

The experimental data in Fig. 4 show also that the meniscus shape is insensitive to the concentration of electrolyte in the aqueous phase. This result implies that (in the investigated system) the electric charges are located at the particle/oil interface, and consequently, the effective dipole moment should be estimated from Eq. (1.2). Using this equation, a value of the surface charge density $\sigma_{pn} = 67.9\ \mu C/m^2$ was determined in Ref. [27]. The latter value is close to the value 80 $\mu C/m^2$, which was obtained in Ref. [39] from the data by Philipse and Vrij [50] for zeta potentials of silanized silica particles in toluene–ethanol mixtures.

In Section 3.3, we will consider the problem about the meniscus shape around two interacting particles separated at a center-to-center distance L. For simplicity, we will assume that the contact lines remain horizontal, as depicted in Fig. 2, at all values of L. Here, we will estimate the accuracy of this approximation.

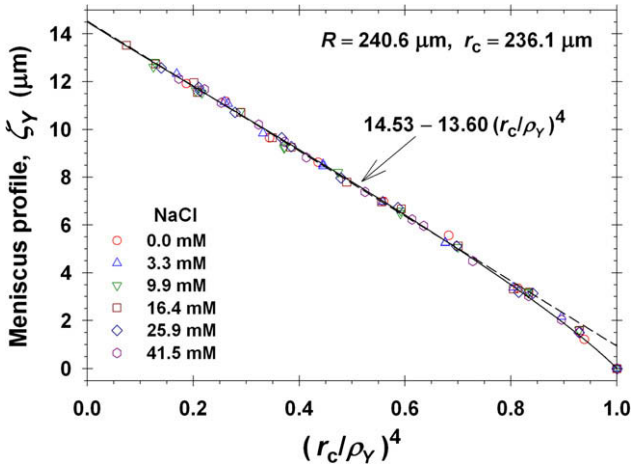

Fig. 4. Plot of the electric interfacial deformation, ζ_Y vs. $(r_c/\rho_Y)^4$ for experimental data form Ref. [27] for a particle of radius $R = 240.6$ μm located at a water/tetradecane interface. The symbols are digitized points from the meniscus profile taken from side-view photographs at various NaCl concentrations in water, which are denoted in the figure. The solid line is a fit by cubic parabola. For $0 < r_c/\rho_Y < 0.96$, the data comply very well with the dashed straight line, whose parameters are shown in the graph.

Under the action of the electric field of the other particle, the plane of the contact line of a given particle might be rotated at an angle β with respect to the horizontal position. This will induce an interfacial deformation that is equivalent to a capillary dipole [6,7,17,51]. The interaction force between two capillary dipoles is given by the following asymptotic expression [51]:

$$F_x \approx -4\pi\gamma h_A h_B \frac{r_c^2}{L^3}, \tag{3.9}$$

where h_A and h_B are the amplitudes of the capillary dipoles. (The cosine that characterizes their mutual orientation is set equal to 1, which corresponds to the energetically most favorable configuration.) The amplitudes are proportional to the force moment, M_E, which is due to the electric field of the other particle: $h_A, h_B \propto M_E$. Further, we have $M_E \propto p_d E_x \propto 1/L^4$; see Fig. 2 and Eq. (3.2). Then, the product of the two amplitudes is $h_A h_B \propto 1/L^8$, and Eq. (3.9) yields $F_x \propto 1/L^{11}$. Because the leading term in F_x is $\propto 1/L^4$, the effect of the contact line inclination turns out to be of considerably higher order and will be neglected in subsequent calculations.

3.3. Meniscus around two particles and calculation of $F_x^{(\gamma)}$

To determine the meniscus profile, $z = \zeta(x, y)$, around two particles (Fig. 2), in the right-hand-side of Eq. (2.8) we substitute $\varphi_n = \varphi_{A,0} + \varphi_{B,0}$ from Eq. (3.2), which leads to:

$$\frac{\partial^2\zeta}{\partial x^2} + \frac{\partial^2\zeta}{\partial y^2} = -\frac{p_d^2}{8\pi\gamma\varepsilon_n}\left(\frac{1}{\rho_A^6} + \frac{2}{\rho_A^3\rho_B^3} + \frac{1}{\rho_B^6}\right). \tag{3.10}$$

One could check that a particular solution to the inhomogeneous Eq. (3.10) is given by the expression:

$$\zeta_{\text{inh}} \equiv -\frac{p_d^2}{128\pi\gamma\varepsilon_n}\left(\frac{1}{\rho_A^4} + \frac{1}{\rho_B^4}\right) + \frac{p_d^2}{4\pi\gamma\varepsilon_n L^2}\left(\frac{1}{\rho_A\rho_B} - 2\frac{\rho_A^2 + \rho_B^2}{\rho_A\rho_B L^2}\right), \tag{3.11}$$

where

$$\rho_A^2 = (x + L/2)^2 + y^2, \quad \rho_B^2 = (x - L/2)^2 + y^2 \tag{3.12}$$

(see Fig. 3). The general solution of Eq. (3.10) represents a sum of $\zeta_{\text{inh}}(x, y)$ and the solution of the respective homogeneous equation, $\zeta_h(x,y)$:

Table 1
Expressions for the coefficients $A_0,\ldots,A_5$ in Eq. (3.16); $\lambda \equiv r_c/L$.

$A_0 = \frac{1}{128} + \frac{\lambda^3}{4} + \frac{\lambda^4}{128} - \frac{3\lambda^5}{16} + \frac{\lambda^6}{16} - \frac{127}{256}\lambda^7 + \frac{31}{128}\lambda^8$
$A_1 = \frac{3}{4}\lambda^4 - \frac{1}{32}\lambda^5 - \frac{19}{32}\lambda^6 - \frac{5}{32}\lambda^7 - \frac{299}{256}\lambda^8$
$A_2 = \frac{7}{16}\lambda^5 + \frac{1}{64}\lambda^6 + \frac{29}{64}\lambda^7 + \frac{1}{32}\lambda^8$
$A_3 = \frac{11}{32}\lambda^6 + \frac{337}{512}\lambda^8$
$A_4 = \frac{75}{256}\lambda^7, \quad A_5 = \frac{133}{512}\lambda^8$

$$\zeta = \zeta_{\rm inh} + \zeta_h \quad \text{where} \quad \frac{\partial^2\zeta_h}{\partial x^2} + \frac{\partial^2\zeta_h}{\partial y^2} = 0. \tag{3.13}$$

Because $\zeta = 0$ at the particle contact lines (see Fig. 2 and the discussion in Section 3.2), we obtain the following boundary condition for ζ_h:

$$\zeta_h = -\zeta_{\rm inh} \quad \text{at } \rho_A = r_c \quad \text{and} \quad \rho_B = r_c, \tag{3.14}$$

where $\zeta_{\rm inh}$ is given by Eq. (3.11). Having determined $\zeta(x,y)$, we can further calculate the x-projection of the interaction force $\mathbf{F}^{(\gamma)}$ acting on the right-hand-side particle by using Eq. (2.6):

$$F_x^{(\gamma)} = -\gamma r_c \int_0^{2\pi} \left[1 + \left(\frac{\partial\zeta}{\partial\rho_B}\right)^2\right]^{-1/2} \cos\phi_B\, d\phi_B$$
$$\approx \frac{\gamma r_c}{2} \int_0^{2\pi} \left(\frac{\partial\zeta}{\partial\rho_B}\right)^2 \cos\phi_B\, d\phi_B \quad \text{at } \rho_B = r_c. \tag{3.15}$$

The fact that the meniscus slope is small has been used; (ρ_B, ϕ_B) are polar coordinates associated with the right-hand-side particle (Fig. 3).

We found the function $\zeta_h(x,y)$ in the form of a truncated Fourier expansion by solving Eq. (3.13) in terms of bipolar coordinates (τ,ω) – see Appendix A for details:

$$\zeta_h = \frac{p_d^2}{\pi\gamma\varepsilon_n r_c^4}\left[A_0 + \sum_{k=1}^{5} A_k \frac{\cosh(k\tau)}{\cosh(k\tau_c)}\cos(k\omega) + O\left(\frac{r_c^9}{L^9}\right)\right]. \tag{3.16}$$

The coefficients $A_0,\ldots,A_5$ are given in Table 1. Next, $\zeta = \zeta_{\rm inh} + \zeta_h$ is substituted in Eq. (3.15) and the integration is carried out. The result is obtained in the form of a series expansion with respect to the powers of r_c/L (see Appendix A):

$$F_x^{(\gamma)} = \frac{p_d^4}{2\pi\gamma\varepsilon_n^2 r_c^9} f_x^{(\gamma)}, \tag{3.17}$$

$$f_x^{(\gamma)} = \frac{3\lambda^4}{64} - \frac{\lambda^5}{256} - \frac{93\lambda^6}{512} + \frac{91\lambda^7}{256} + \frac{\lambda^8}{4096} + O(\lambda^9), \tag{3.18}$$

where $\lambda \equiv r_c/L$. The positive sign of the first term in the right-hand-side of Eq. (3.18) means that at long interparticle distances, $F_x^{(\gamma)}$ corresponds to *repulsion*. To determine the total interaction force, we have to calculate also $F_x^{(p)}$ (see Section 4.1).

4. Calculation of $F_x^{(p)}$ and of the total force F_x

4.1. Calculation of $F_x^{(p)}$

The force experienced by a dipole of moment $\mathbf{p}$ is $\mathbf{F} = \mathbf{p}\cdot\nabla\mathbf{E}$, where $\mathbf{E}$ is the applied external electric field (the field of the considered dipole $\mathbf{p}$ being excluded) [48,52]. With $\mathbf{p} = p_d\mathbf{e}_z$ and $\mathbf{E} = -\nabla(\varphi_{A,0} + \varphi_1)$, we find the x-projection of the force $\mathbf{F}^{(p)}$ acting on the particle B:

$$F_x^{(p)} = -\frac{p_d}{2}\frac{\partial}{\partial z}\left(\frac{\partial\varphi_{A,0}}{\partial x} + \frac{\partial\varphi_1}{\partial x}\right) = \frac{3p_d^2}{2\varepsilon_n L^4} - \frac{p_d}{2}\frac{\partial^2\varphi_1}{\partial x\partial z}\bigg|_{x=L/2, y=z=0}, \tag{4.1}$$

where we have substituted $\varphi_{A,0}$ from Eq. (3.2). In Eq. (4.1), the factor 1/2 appears because the electric field is present only in the upper half-space (Fig. 1). To calculate $F_x^{(p)}$, we have to first determine φ_1. We recall that φ_1 originates from the interfacial deformation, and satisfies the Laplace equation $\nabla^2\varphi_1 = 0$ along with the boundary condition, Eq. (2.10).

At a given boundary condition for φ_1 in the plane $z = 0$, we can calculate φ_1 in the upper half-space ($z > 0$) by using the known Green function for the Dirichlet boundary problem:

$$\varphi_1(x,y,z) = \frac{1}{2\pi}\int_{-\infty}^{\infty}\int_{-\infty}^{\infty} \frac{z\varphi_s(\tilde{x},\tilde{y})}{\left[(x-\tilde{x})^2 + (y-\tilde{y})^2 + z^2\right]^{3/2}}\, d\tilde{x}\, d\tilde{y}, \tag{4.2}$$

where $\tilde{x}$ and $\tilde{y}$ are integration variables. In view of Eq. (2.10), the function φ_s is defined as follows:

$$\varphi_s = -\zeta\frac{\partial\varphi_0}{\partial z}\bigg|_{z=0}. \tag{4.3}$$

The definition of ζ is extended as $\zeta \equiv 0$ in the circles $\rho_A \leqslant r_c$ and $\rho_B \leqslant r_c$ (Fig. 2), which gives $\varphi_s = 0$ in the same circles; see Eq. (4.3). In Eqs. (4.2) and (4.3), φ_0 can be substituted from Eqs. (3.1) and (3.2), and $\zeta(x,y)$ – from Eqs. (3.11), (3.13) and (3.16). As a result, from Eqs. 4.1, 4.2 and 4.3 we obtain an expression for $F_x^{(p)}$ in the form of series expansion (Appendix B):

$$F_x^{(p)} = \frac{3p_d^2}{2\varepsilon_n L^4} + \frac{p_d^4}{2\pi\gamma\varepsilon_n^2 r_c^9} f_x^{(p)}, \tag{4.4}$$

$$f_x^{(p)} = -\frac{27\lambda^4}{320} + \frac{\lambda^5}{256} + \frac{213}{512}\lambda^6 - \frac{271}{256}\lambda^7 + \frac{2099}{4096}\lambda^8 + o(\lambda^8), \tag{4.5}$$

where $\lambda \equiv r_c/L$. Combining Eqs. (3.17), (3.18) and (4.4), (4.5), we finally obtain an expression for the total interaction force, F_x, acting on the right-hand-side particle B, in the form of a series expansion:

$$F_x = \frac{3p_d^2}{2\varepsilon_n L^4}\left[1 - \frac{2\delta}{5} + \frac{5\delta}{2}\left(\frac{r_c}{L}\right)^2 - \frac{15\delta}{2}\left(\frac{r_c}{L}\right)^3 + \frac{175\delta}{32}\left(\frac{r_c}{L}\right)^4 + \cdots\right]. \tag{4.6}$$

Here, $\delta = \tan\psi_c$ is the meniscus slope at the contact line given by Eq. (3.5).

4.2. Summary and discussion

The first term in the brackets in Eq. (4.6) corresponds to the force of direct electric repulsion, F_{ER}, between two charged particles adsorbed at a planar liquid interface ($\delta = 0$); see Eq. (1.1). Hence, the sum of all other terms in Eq. (4.6) (those $\propto \delta$) gives the electrocapillary force:

$$F_{EC} = -\frac{3p_d^2\delta}{2\varepsilon_n L^4}\left[\frac{2}{5} - \frac{5}{2}\left(\frac{r_c}{L}\right)^2 + \frac{15}{2}\left(\frac{r_c}{L}\right)^3 - \frac{175}{32}\left(\frac{r_c}{L}\right)^4 + \cdots\right]. \tag{4.7}$$

Note that a term $\propto r_c/L$ is missing in the brackets in Eq. (4.7), and hence the higher-order terms represent small corrections to the leading term 2/5. Despite the fact that the leading term in $f_x^{(\gamma)}$ is positive (repulsive), see Eq. (3.18), the electrocapillary force F_{EC} is negative (attractive) thanks to the contribution from the leading term in $f_x^{(p)}$; see Eq. (4.5). In view of Eq. (1.1), taking the leading term in Eq. (4.7) we obtain:

$$\frac{|F_{EC}|}{|F_{ER}|} \approx \frac{2}{5}\tan\psi_c \quad \text{for } \left(\frac{r_c}{L}\right)^2 \ll 1, \tag{4.8}$$

where the relation $\delta = \tan\psi_c$ has been used. Because we are working at small meniscus slope, we have $\tan\psi_c < 1$, which means that $|F_{EC}| < |F_{ER}|$. In other words, the total force, $F_x = F_{ER} + F_{EC}$ is positive (repulsive); see Eq. (4.6). Thus, in the region where the asymptotic expansion, Eq. (4.6) is applicable, the electrostatic repulsion between the two like-charged particles prevails over the capillary attraction. Note, however, that in other cases (anisotropic surface charge distribution) the capillary attraction may prevail [35]. In

Fig. 5a, the dependencies of $|F_{EC}|$ and F_{ER} on the interparticle distance L are compared at $\psi_c = 15°$. In view of Eq. (4.8), at other ψ_c values the relative magnitude of F_{ER} varies $\propto \tan\psi_c$. One sees that $|F_{EC}|$ is of the order of 10% of F_{ER} (Fig. 5a).

Having in mind that the electrodipping force is given by the expression $F_{ED} = 2\pi\gamma r_c \sin\psi_c$, and that $\sin\psi_c \approx \tan\psi_c$ at small meniscus slopes, we obtain an asymptotic relation between F_{ER}, F_{EC} and F_{ED}:

$$\frac{|F_{EC}|}{|F_{ER}|} \approx \frac{|F_{ED}|}{5\pi\gamma r_c} \quad \text{for } \left(\frac{r_c}{L}\right)^2 \ll 1. \tag{4.9}$$

Using Eqs. (1.1), (2.5) and (4.4), we can express the electrocapillary force, F_{EC}, in the form:

$$F_{EC} = F_x^{(\gamma)} + F_x^{(p,\delta)}. \tag{4.10}$$

where $F_x^{(\gamma)}$ is a contribution from the integral of surface tension γ along the particle contact line (Fig. 1), and by definition

$$F_x^{(p,\delta)} \equiv F_x^{(p)} - F_{ER} \tag{4.11}$$

i.e. $F_x^{(p,\delta)}$ is equal to the integral of the pressure tensor over the particle surface minus the force of direct electrostatic repulsion, F_{ER}. In view of Eqs. (3.5) and (4.4), $F_x^{(p,\delta)} \propto \delta = \tan\psi_c$, and hence $F_x^{(p,\delta)}$ would be equal to zero in the absence of interfacial deformation ($\delta = 0$).

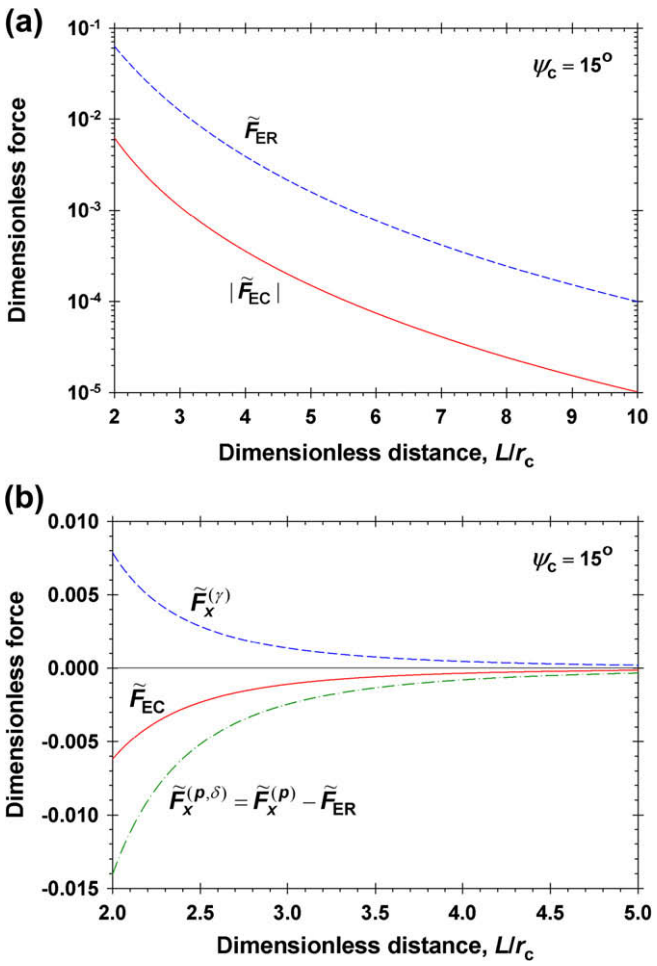

Fig. 5. (a) Plots of the dimensionless electrostatic repulsion, $\widetilde{F}_{ER}$, and electrocapillary attraction, $|\widetilde{F}_{EC}|$, vs. the dimensionless interparticle distance L/r_c, calculated from Eqs. (1.1) and (4.7). (b) Plots of $\widetilde{F}_{EC}$, $\widetilde{F}_x^{(\gamma)}$ and $\widetilde{F}_x^{(p,\delta)}$ vs. L/r_c, calculated by using Eqs. (3.5), (3.17), (3.18), (4.4), (4.5) and (4.11). The meniscus slope angle at the contact line is $\psi_c = 15°$. The tilde means that the respective force is scaled with $3p_d^2/(2\varepsilon_n r_c^4)$.

The forces $F_x^{(\gamma)}$, $F_x^{(p,\delta)}$ and F_{EC} are compared in Fig. 5b. One sees that $F_x^{(\gamma)}$ is positive (repulsive), $F_x^{(p,\delta)}$ is negative (attractive), and their sum, F_{EC}, is attractive because the effect of pressure, $F_x^{(p,\delta)}$, is predominant in Eq. (4.10). In this respect, the situation is different from the case of gravity-induced capillary force, where the pressure contribution is negligible for sub-millimeter particles, whereas the surface tension integral, $F_x^{(\gamma)}$, corresponds to attraction [4,16]. This difference originates from the fact that the presence of gravitational and electric fields lead to the appearance of different terms (with different functional dependences) in the Young–Laplace equation (see e.g. Eq. (3.10)), which results in different meniscus shapes.

4.3. The total force as interaction between effective dipoles

Let us consider the left-hand-side particle in isolation (i.e. at $L \to \infty$). In this case $\varphi_{n,0} = \varphi_{A,0}$, the meniscus profile ζ_A is given by Eq. (3.7), and then Eq. (4.3) acquires the form:

$$\varphi_s = -\frac{p_d^3}{128\pi\gamma\varepsilon_n^2}\left(\frac{1}{r_c^4} - \frac{1}{\rho_A^4}\right)\frac{1}{\rho_A^3} \quad \text{for } \rho_A > r_c, \tag{4.12}$$

$$\varphi_s = 0 \quad \text{for } \rho_A \leqslant r_c. \tag{4.13}$$

Substituting Eqs. (4.12) and (4.13) into Eq. (4.2), we obtain the following expression for the correction term in the electrostatic potential:

$$\varphi_{A,1}\left(-\frac{L}{2}, 0, z\right) = -\frac{p_d r_c^5 \delta}{4\varepsilon_n}\int_{r_c}^{\infty}\left(\frac{1}{r_c^4} - \frac{1}{\rho_A^4}\right)\frac{1}{\rho_A^2}\frac{z d\rho_A}{(\rho_A^2 + z^2)^{3/2}}. \tag{4.14}$$

In Eq. (4.12), γ has been eliminated using the definition of δ, Eq. (3.5). Eq. (4.14) is written at the axis of revolution of particle A, and correspondingly, we have set $x = -L/2$ and $y = 0$ in Eq. (4.2). The integral in the right-hand-side of Eq. (4.14) can be solved analytically:

$$\varphi_{A,1}\left(-\frac{L}{2}, 0, z\right) = -\frac{p_d\delta}{\varepsilon_n(z^2 + r_c^2)^{1/2}} \times \left[\frac{1}{5z} + \frac{3r_c^2}{5z^3} - \frac{2r_c^4}{5z^5} - \frac{4r_c^6}{5z^7} - \left(\frac{r_c}{2z^3} - \frac{4r_c^5}{5z^7}\right)(z^2 + r_c^2)^{1/2}\right]. \tag{4.15}$$

By using series expansion at small z, one can check that $\varphi_{A,1}(-L/2, 0, z) \to 0$ at $z \to 0$. i.e. the divergent terms in Eq. (4.15) at $z \to 0$ cancel each other. In the other limit, $z \to \infty$, the series expansion of Eq. (4.15) reads:

$$\varphi_{A,1}\left(-\frac{L}{2}, 0, z\right) = \frac{p_d\delta}{\varepsilon_n}\left(-\frac{1}{5z^2} + \frac{r_c}{2z^3} + \cdots\right). \tag{4.16}$$

Combining Eqs. (2.9), (3.2) and (4.16), we obtain the following series for the electrostatic potential at the axis of revolution:

$$\varphi_A\left(-\frac{L}{2}, 0, z\right) = \frac{p_d}{\varepsilon_n z^2}\left(1 - \frac{\delta}{5} + \frac{r_c\delta}{2z} + \cdots\right) = \frac{\tilde{p}_d}{\varepsilon_n z^2}\left[1 + O\left(\frac{r_c\delta}{2z}\right)\right], \tag{4.17}$$

where

$$\tilde{p}_d \equiv p_d\left(1 - \frac{\delta}{5}\right). \tag{4.18}$$

The above result implies that the electric field far from the particle (for $z \gg r_c\delta/2$) behaves as a dipole with an effective dipole moment $\tilde{p}_d$, which is smaller than the original dipole moment p_d (at flat liquid interface). This is due to the formation of meniscus around the particle, which is taken into the account by the correction term φ_1 in Eq. (4.2). In terms of the effective dipole moment $\tilde{p}_d$, Eq. (4.6) acquires the form:

$$F_x = \frac{3\tilde{p}_d^2}{2\varepsilon_n L^4}\left[1 + O\left(\frac{r_c^2\delta}{L^2}\right)\right]. \tag{4.19}$$

Because we are working at small meniscus slope, $\delta^2 \ll 1$, terms of the order of δ^2 (and higher-order terms) have been neglected everywhere in this article. Eq. (4.19) shows that the force of interaction between two charged particles at a water/nonpolar-fluid interface can be considered as interaction between two electric dipoles of effective dipole moment $\tilde{p}_d$. The capillary effect influences the interaction through the term $\delta/5$ in Eq. (4.18). This term diminishes the effective dipole moment of the particle and the net repulsion between two similar particles, which is equivalent to the effect of the electrocapillary attraction; see Eq. (4.7).

The forces between colloidal spheres (of diameter 3.1 μm) at a decane-water interface, in the presence of low concentrations of NaCl and the ionic surfactant sodium dodecyl sulfate (SDS) in the aqueous subphase, have been studied using laser tweezers [33]. The experimental data indicate interparticle repulsion $F_x \propto 1/L^4$, in agreement with Eq. (4.19). The increase of both NaCl and SDS concentrations leads to decrease of the magnitude of the measured F_x. This effect can be explained with a partial screening of surface charges at the particle/water interface with the rise of the ionic strength of the aqueous solution. As a result, the electric field of these charges, which penetrates through the dielectric particles in the nonpolar fluid, becomes weaker, i.e. the effective dipole moment $\tilde{p}_d$ decreases. It should be noted that the increase of the ionic strength leads to diminishing of the Debye screening length, κ^{-1}, which makes our theory applicable to sub-micrometer particles. As already mentioned, for very small particles, for which the particle radius is comparable with κ^{-1}, the screened coulomb repulsion becomes significant at short interparticle separations, in addition to the dipole repulsion [37,38,44].

The final conclusion from our detailed analysis is that the direct electrostatic repulsion dominates over the capillary attraction when the surface charge is uniformly distributed; no matter whether the surface charge is on the polar-liquid or nonpolar-fluid side of the particle.

Electric-field-induced attraction that prevails over the electrostatic repulsion was established (both experimentally and theoretically) in the case of not-too-small floating particles, for which the interfacial deformation due to gravity is not negligible [34,35]. If the surface charge is anisotropically distributed (this may happen at low surface charge density), the electric field produces a saddle-shaped deformation in the liquid interface near the particle, which is equivalent to a "capillary quadrupole". The interaction of the latter with the axisymmetric gravitational deformation around the other particle (which is equivalent to a "capillary charge") gives rise to a capillary force that decays $\propto 1/L^3$, i.e. slower than $F_{ER} \propto 1/L^4$. In such a case, we are dealing with a *hybrid* interaction between a gravity-induced "capillary charge" and an electric-field-induced capillary quadrupole [35]. This effect cannot explain the effective attraction registered in Ref. [1], where the particles are rather small, and the gravity-induced interfacial deformation is negligible. Recent reviews on the forces between capillary multipoles can be found in Refs. [23,53].

5. Concluding remarks

Charged particles adsorbed at a liquid interface experience the action of several forces (Fig. 1). First, the electrodipping force is pushing each separate particle toward the fluid phase of greater dielectric constant, usually – the water phase. Second, like-charged particles experience a direct electric repulsion. In addition, the particle electric field gives an electrostatic contribution to pressure, which leads to the appearance of an electric-field induced deformation (capillary meniscus) in the liquid interface around each particle. The overlap of such deformations produces an electrocapillary force of interaction between the particles. Our goal in the present article is to quantify this interaction on the basis of a force approach, which is different from the approaches (mostly based on energy calculations) used by other authors. The fact that the electric field of adsorbed particles behaves asymptotically as a field of a dipole is utilized to derive analytical expressions for the meniscus profile; see Eqs. (3.11), (3.13), (3.16) and Table 1. The comparison of the calculated profile with experimental data indicates that the result based on the dipolar approximation agrees excellently with the data, except some small deviations near the contact line (Fig. 4). The effect of the interfacial deformation on the electrostatic pressure is also taken into account; see Eqs. (2.10) and (4.2). The two-particle electrocapillary problem is solved in bipolar coordinates without using the superposition approximation (Appendices A and B). The derived expression for the electrocapillary attraction shows that it is weaker that the electrostatic repulsion at all interparticle distances at which the dipolar approximation is applicable; see Eqs. (4.6), (4.7) and (4.8). This result is in agreement with the conclusions of other authors obtained by using different theoretical approaches [29,32] and with available experimental data [33]. The analytical expressions for the electrodipping and electrocapillary forces derived in the present article provide a simple and convenient way for estimation of the magnitude of these forces.

Acknowledgments

Support from the National Science Fund of Bulgaria, Grant Number DO-02-121/2009, and a partial support from EU COST Action D43 "Colloid and Interface Chemistry for Nanotechnology" are gratefully acknowledged. The authors thank Ms. Mariana Paraskova for her assistance in the figure preparation.

Appendix A. Surface–tension contribution to the interaction force, $F_x^{(\gamma)}$

The meniscus profile $z = \zeta(x, y)$, which satisfies Eq. (3.10), can be presented in the form $\zeta = \zeta_{\rm inh} + \zeta_h$, where $\zeta_{\rm inh}$ is a particular solution to the inhomogeneous equation given by Eq. (3.11), and ζ_h is the solution of the homogeneous Eq. (3.13). Our goal is to find ζ_h and then to calculate $F_x^{(\gamma)}$ by carrying out the integration in Eq. (3.15). For this goal, it is convenient to introduce bipolar coordinates (τ, ω) in the xy-plane:

$$x \equiv \frac{a}{u}\sinh\tau, \quad y \equiv \frac{a}{u}\sin\omega, \tag{A.1}$$

$$u \equiv \cosh\tau - \cos\omega. \tag{A.2}$$

Here, u is a metric coefficient and a is a parameter, which is to be determined from the boundary conditions; see Eq. (A.3). The coordinate lines $\tau = \text{const.}$ and $\omega = \text{const.}$ are two families of mutually orthogonal circumferences (see Fig. 6). We determine a in such a way that the contact lines of the two particles to correspond to the coordinate circumferences $\tau = \tau_c$ and $\tau = -\tau_c$:

$$\frac{a}{r_c} = \sinh\tau_c = \left(\frac{L^2}{4} - r_c^2\right)^{1/2}, \quad \cosh\tau_c = \frac{L}{2r_c}, \quad \text{and}$$

$$\tau_c = \ln\left(\frac{L + 2a}{2r_c}\right). \tag{A.3}$$

See also Fig. 3. In bipolar coordinates, Eq. (3.13) acquires the form:

$$\frac{\partial^2\zeta_h}{\partial\tau^2} + \frac{\partial^2\zeta_h}{\partial\omega^2} = 0. \tag{A.4}$$

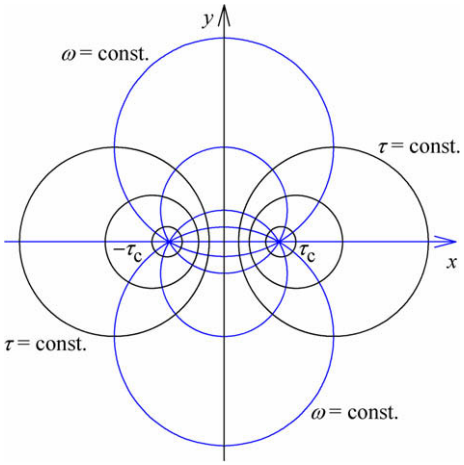

Fig. 6. Bipolar coordinates (τ,ω) in the xy-plane. The $\tau=$ const. and $\omega=$ const. coordinate lines represent two families of mutually orthogonal circumferences. The contact lines on the particle surfaces correspond to $\tau=\pm\tau_c$.

Because of the symmetry of the considered problem, at the mid-plane $x=0$ we have:

$$\frac{\partial\zeta_{h,0}}{\partial\tau}=0 \quad \text{at } \tau=0. \tag{A.5}$$

At the contact line $\rho_B=r_c$ of the right-hand-side particle, we should have $\zeta_h=-\zeta_{\rm inh}$. In view of Eq. (3.11), we obtain the following boundary condition:

$$\zeta_h|_{\rho_B=r_c}=\frac{p_d^2}{128\pi\gamma\varepsilon_n}\left(\frac{1}{\rho_A^4}+\frac{1}{r_c^4}\right)-\frac{p_d^2}{4\pi\gamma\varepsilon_n L^2}\left(\frac{1}{\rho_A r_c}-2\frac{\rho_A^2+r_c^2}{\rho_A r_c L^2}\right), \tag{A.6}$$

In addition, at $\rho_B=r_c$ the distance ρ_A can be expressed as a function of ω:

$$\rho_A|_{\rho_B=r_c}=\left[\frac{1-3(r_c/L)^2-2(r_c/L)^3\cos\omega}{1-2(r_c/L)\cos\omega}\right]^{1/2}L. \tag{A.7}$$

Next, we expand Eqs. (A.6) and (A.7) in series for $r_c/L\ll 1$, and after that the result is expanded in Fourier series in terms of ω. The final result reads:

$$\zeta_h|_{\rho_B=r_c}=\frac{p_d^2}{\pi\gamma\varepsilon_n r_c^4}\left[\sum_{k=0}^{5}A_k\cos(k\omega)+O\left(\frac{r_c^9}{L^9}\right)\right], \tag{A.8}$$

where the dimensionless coefficients $A_0,\ldots,A_5$ are given in Table 1. The solution of Eq. (A.4), along with the boundary conditions, Eqs. (A.5) and (A.8), is:

$$\zeta_{h,0}=\frac{p_A^2}{\pi\gamma\varepsilon_n r_c^4}\left[A_0+\sum_{k=1}^{5}A_k\frac{\cosh(k\tau)}{\cosh(k\tau_c)}\cos(k\omega)+O\left(\frac{r_c^9}{L^9}\right)\right]. \tag{A.9}$$

Using the identity

$$\cos\phi_B=\frac{1-\cosh\tau_c\cos\omega}{\cosh\tau_c-\cos\omega}, \tag{A.10}$$

we bring Eq. (3.15) in the form:

$$F_x^{(\gamma)}=\frac{\gamma}{2r_c}\left(1-\frac{4r_c^2}{L^2}\right)^{-1/2}\int_0^{2\pi}\left(\frac{\partial\zeta}{\partial\tau}\right)^2\left(\frac{2r_c}{L}-\cos\omega\right)d\omega \quad \text{at } \tau=\tau_c. \tag{A.11}$$

It is convenient to introduce the dimensionless variable $\tilde\zeta$ as follows:

$$\tilde\zeta=\frac{\pi\gamma\varepsilon_n r_c^4}{p_d^2}\zeta. \tag{A.12}$$

In view of Eq. (3.17) and (A.12), Eq. (A.11) acquires the form:

$$f_x^{(\gamma)}\equiv\frac{1}{\pi}\left(1-\frac{4r_c^2}{L^2}\right)^{-1/2}\int_0^{2\pi}\left(\frac{\partial\tilde\zeta}{\partial\tau}\right)^2\left(\frac{2r_c}{L}-\cos\omega\right)d\omega \quad \text{at } \tau=\tau_c. \tag{A.13}$$

Having in mind that $\zeta=\zeta_{\rm inh}+\zeta_h$, with the help of Eqs. (3.11), (A.9), (A.12) and (A.13), we obtain an asymptotic expression for the dimensionless meniscus profile:

$$\begin{aligned}\tilde\zeta=&-\frac{1}{128}\left[\frac{\cosh\tau-\cos\omega}{\cosh(\tau+2\tau_c)-\cos\omega}\right]^2-\frac{1}{128}\left[\frac{\cosh\tau-\cos\omega}{\cosh(\tau-2\tau_c)-\cos\omega}\right]^2-\frac{\sinh^2\tau_c}{16\cosh^4\tau_c}\\&\times\frac{\cosh\tau+\cos\omega}{\{[\cosh(\tau+2\tau_c)-\cos\omega][\cosh(\tau-2\tau_c)-\cos\omega]\}^{1/2}}\\&+A_0+\sum_{k=1}^{5}A_k\frac{\cosh(k\tau)}{\cosh(k\tau_c)}\cos(k\omega)+O\left(\frac{r_c^9}{L^9}\right).\end{aligned} \tag{A.14}$$

Differentiating Eq. (A.14) with respect to τ , we derive:

$$\begin{aligned}\left.\frac{\partial\tilde\zeta}{\partial\tau}\right|_{\tau=\tau_c}=&-\frac{1}{32}\frac{\sinh\tau_c}{\cosh\tau_c-\cos\omega}-\frac{1}{64}\\&\times\frac{(\cosh\tau_c-\cos\omega)\sinh\tau_c}{[\cosh(3\tau_c)-\cos\omega]^2}+\frac{1}{64}\\&\times\frac{(\cosh\tau_c-\cos\omega)^2\sinh(3\tau_c)}{[\cosh(3\tau_c)-\cos\omega]^3}-\frac{\sinh^3\tau_c}{8\cosh^2\tau_c}\\&\times\frac{\cosh(2\tau_c)-\sin^2\omega-\cosh\tau_c\cos\omega}{[\cosh(3\tau_c)-\cos\omega]^{3/2}(\cosh\tau_c-\cos\omega)^{3/2}}\\&+\sum_{k=1}^{5}kA_k\frac{\sinh(k\tau_c)}{\cosh(k\tau_c)}\cos(k\omega)+O\left(\frac{r_c^9}{L^9}\right).\end{aligned} \tag{A.15}$$

Further, we expand Eq. (A.15) in series for $r_c/L\ll 1$. The result reads:

$$\left.\frac{\partial\tilde\zeta}{\partial\tau}\right|_{\tau=\tau_c}=\sum_{k=0}^{8}B_k\cos(k\omega)+O\left(\frac{r_c^9}{L^9}\right), \tag{A.16}$$

where the dimensionless coefficients, $B_0,\ldots,B_8$, are expressed as power series of the small parameter $\lambda\equiv r_c/L$ neglecting terms of order higher than λ^8:

$$\begin{aligned}B_0&=-\frac{1}{32}-\frac{\lambda^3}{4}+\frac{9\lambda^5}{16}+\frac{\lambda^6}{16}+\frac{75\lambda^7}{256}+\frac{9\lambda^8}{32},\\B_1&=-\frac{\lambda}{16}-\frac{\lambda^3}{16}+\frac{\lambda^4}{4}-\frac{3\lambda^5}{16}-\frac{67}{32}\lambda^6-\frac{5}{8}\lambda^7-\frac{237}{256}\lambda^8,\\B_2&=-\frac{\lambda^2}{16}-\frac{\lambda^4}{8}+\frac{\lambda^5}{16}-\frac{\lambda^6}{4}+\frac{33}{64}\lambda^7-\frac{3}{4}\lambda^8,\\B_3&=-\frac{\lambda^3}{16}-\frac{3\lambda^5}{16}+\frac{\lambda^6}{32}-\frac{9\lambda^7}{16}+\frac{105}{512}\lambda^8,\\B_4&=-\frac{\lambda^4}{16}-\frac{\lambda^6}{4}+\frac{5\lambda^7}{256}-\frac{7}{8}\lambda^8,\\B_5&=-\frac{\lambda^5}{16}-\frac{5\lambda^7}{16}+\frac{7\lambda^8}{512},\\B_6&=-\frac{1}{16}\lambda^6-\frac{3}{8}\lambda^8,\\B_7&=-\frac{\lambda^7}{16},\quad B_8=-\frac{\lambda^8}{16}.\end{aligned}$$

Substituting Eq. (A.16) in the right-hand-side of Eq. (A.13), we obtain Eq. (3.17) in the main text.

Appendix B. Pressure contribution to the interaction force, $F_x^{(p)}$

Substituting Eq. (4.2), into the right-hand-side of Eq. (4.1) we obtain:

$$F_x^{(p)} = \frac{3p_d^2}{2\varepsilon_n L^4} + \frac{3p_d}{4\pi}\int_{-\infty}^{\infty}\int_{-\infty}^{\infty}\frac{L-2x}{2\rho_B^5}\varphi_s(x,y)\,dx\,dy. \tag{B.1}$$

Furthermore, substituting φ_s from Eq. (4.3) and using Eqs. (3.1), (3.2), and (A.12), we derive Eq. (4.4), where the dimensionless force coefficient $f_x^{(p)}$ is defined as follows:

$$f_x^{(p)} \equiv \frac{3r_c^5}{4\pi}\int_{-\infty}^{\infty}\int_{-\infty}^{\infty}\left(\frac{1}{\rho_A^3}+\frac{1}{\rho_B^3}\right)\frac{2x-L}{\rho_B^5}\tilde{\zeta}\,dx\,dy. \tag{B.2}$$

The integral in Eq. (B.2) is taken over the region $\rho_A \geqslant r_c$ and $\rho_B \geqslant r_c$; see Eq. (3.12) for the definitions of ρ_A and ρ_B. The meniscus shape is symmetric with respect to the plane $x = 0$, and consequently

$$\int_{-\infty}^{0}\left(\frac{1}{\rho_A^3}+\frac{1}{\rho_B^3}\right)\frac{2x-L}{\rho_B^5}\tilde{\zeta}dx = -\int_{0}^{\infty}\left(\frac{1}{\rho_A^3}+\frac{1}{\rho_B^3}\right)\frac{2x+L}{\rho_A^5}\tilde{\zeta}\,dx. \tag{B.3}$$

Using Eq. (B.3), we rearrange Eq. (B.2) into a symmetric form:

$$f_x^{(p)} = -\frac{3r_c^5}{4\pi}\int_{-\infty}^{\infty}dy \times\int_0^{\infty}dx\left[\frac{L+2x}{\rho_A^8}+\frac{L-2x}{\rho_B^8}+\frac{L(4y^2-4x^2+L^2)}{2\rho_A^5\rho_B^5}\right]\tilde{\zeta}. \tag{B.4}$$

Let us consider the function

$$w \equiv \frac{L+2x}{24\rho_A^6}+\frac{L-2x}{24\rho_B^6} + \frac{2\rho_A^2+2\rho_B^2-L^2}{3L^5\rho_A\rho_B}\left[16+\frac{L(L+2x)}{\rho_A^2}+\frac{L(L-2x)}{\rho_B^2}\right]. \tag{B.5}$$

Differentiating $w(x,y)$, we obtain:

$$\nabla^2 w = \frac{L+2x}{\rho_A^8}+\frac{L-2x}{\rho_B^8}+\frac{L(4y^2-4x^2+L^2)}{2\rho_A^5\rho_B^5}, \tag{B.6}$$

where ∇^2 is the Laplace operator in the xy-plane. The combination of Eqs. (B.4) and (B.6) yields:

$$f_x^{(p)} = -\frac{3r_c^5}{4\pi}\int_{-\infty}^{\infty}dy\int_0^{\infty}dx\tilde{\zeta}\nabla^2 w. \tag{B.7}$$

With the help of the two-dimensional divergence theorem, we derive:

$$\begin{aligned}\int_{-\infty}^{\infty}dy\int_0^{\infty}dx(\tilde{\zeta}\nabla^2 w - w\nabla^2\tilde{\zeta}) &= \int_{-\infty}^{\infty}dy\int_0^{\infty}dx[\nabla\cdot(\tilde{\zeta}\nabla w)-\nabla\cdot(w\nabla\tilde{\zeta})]\\ &= -\int_{-\infty}^{\infty}\left(\tilde{\zeta}\frac{\partial w}{\partial x}-w\frac{\partial\tilde{\zeta}}{\partial x}\right)\Big|_{x=0}dy\\ &\quad - r_c\int_0^{2\pi}\left(\tilde{\zeta}\frac{\partial w}{\partial\rho_B}-w\frac{\partial\tilde{\zeta}}{\partial\rho_B}\right)\Big|_{\rho_B=r_c}d\phi_B.\end{aligned} \tag{B.8}$$

The symmetry of the functions $\tilde{\zeta}(x,y)$ and $w(x,y)$ implies that the integral along the y-axis is zero. Then, because $\tilde{\zeta}|_{\rho_B=r_c} = 0$, Eq. (B.8) reduces to:

$$\int_{-\infty}^{\infty}dy\int_0^{\infty}dx\tilde{\zeta}\nabla^2 w = \int_{-\infty}^{\infty}dy\int_0^{\infty}dx w\nabla^2\tilde{\zeta} + r_c \times\int_0^{2\pi}\left(w\frac{\partial\tilde{\zeta}}{\partial\rho_B}\right)\Big|_{\rho_B=r_c}d\phi_B. \tag{B.9}$$

With the help of Eq. (B.9), we represent Eq. (B.7) in the form:

$$f_x^{(p)} = I_1 + I_2, \tag{B.10}$$

$$I_1 \equiv -\frac{3r_c^6}{4\pi}\int_0^{2\pi}\left(w\frac{\partial\tilde{\zeta}}{\partial\rho_B}\right)\Big|_{\rho_B=r_c}d\phi_B, \tag{B.11}$$

$$I_2 \equiv -\frac{3r_c^5}{4\pi}\int_{-\infty}^{\infty}dy\int_0^{\infty}dx w\nabla^2\tilde{\zeta}. \tag{B.12}$$

To calculate I_1, is convenient to introduce bipolar coordinates (see Appendix A):

$$I_1 = \frac{3}{4\pi}\int_0^{2\pi}\left(r_c^5 w\frac{\partial\tilde{\zeta}}{\partial\tau}\right)\Big|_{\tau=\tau_c}d\omega. \tag{B.13}$$

Expanding Eq. (B.5) in series for small values of r_c/L, we obtain:

$$r_c^5 w|_{\tau=\tau_c} = \sum_{k=0}^{9}U_k\cos(k\omega)+O\left(\frac{r_c^9}{L^9}\right), \tag{B.14}$$

where the dimensionless coefficients, $U_0,\ldots,U_9$, are expressed as power series of the small parameter $\lambda \equiv r_c/L$ neglecting terms of order higher than λ^8:

$$\begin{aligned}U_0 &= \frac{\lambda}{12}+\frac{\lambda^3}{12}+\frac{17}{3}\lambda^4+\frac{\lambda^5}{4}-\frac{83}{24}\lambda^6+\frac{4}{3}\lambda^7-\frac{1933}{192}\lambda^8,\\ U_1 &= -\frac{\lambda}{12}+\frac{\lambda^2}{12}-\frac{2}{3}\lambda^3+\frac{\lambda^4}{6}+\frac{227}{12}\lambda^5-\frac{1027}{96}\lambda^7-\frac{5}{3}\lambda^8,\\ U_2 &= -\frac{\lambda}{12}-\frac{5}{3}\lambda^4+\frac{\lambda^5}{12}+\frac{23}{2}\lambda^6+\frac{2}{3}\lambda^7+\frac{6235}{384}\lambda^8,\\ U_3 &= -\frac{\lambda^2}{12}-\frac{\lambda^4}{12}-\frac{9}{4}\lambda^5-\frac{\lambda^6}{12}+\frac{499}{64}\lambda^7-\frac{\lambda^8}{12},\\ U_4 &= -\frac{\lambda^3}{12}-\frac{\lambda^5}{6}-\frac{65}{24}\lambda^6-\frac{\lambda^7}{3}+\frac{757}{192}\lambda^8,\\ U_5 &= -\frac{\lambda^4}{12}-\frac{\lambda^6}{4}-\frac{595}{192}\lambda^7-\frac{2}{3}\lambda^8,\\ U_6 &= -\frac{\lambda^5}{12}-\frac{\lambda^7}{3}-\frac{441}{128}\lambda^8,\quad U_7 = -\frac{\lambda^6}{12}-\frac{5\lambda^8}{12},\\ U_8 &= -\frac{1}{12}\lambda^7,\quad U_9 = -\frac{1}{12}\lambda^8.\end{aligned}$$

Substituting Eqs. (A.16) and (B.14) into Eq. (B.13), we drive:

$$I_1 = -\frac{9\lambda^4}{32}-\frac{111}{256}\lambda^6-\frac{577}{256}\lambda^7-\frac{327}{2048}\lambda^8+O(\lambda^9). \tag{B.15}$$

To calculate the integral I_2, we present Eq. (3.10) in dimensionless form using Eq. (A.12):

$$\nabla^2\tilde{\zeta} = -\frac{r_c^4}{8\rho_A^6}-\frac{r_c^4}{8\rho_B^6}-\frac{r_c^4}{4\rho_A^3\rho_B^3}. \tag{B.16}$$

Substituting Eq. (B.16) in Eq. (B.12), we obtain:

$$I_2 = \frac{3r_c^9}{32\pi}\int_{-\infty}^{\infty}dy\int_0^{\infty}dx\left(\frac{1}{\rho_A^3}+\frac{1}{\rho_B^3}\right)^2 w. \tag{B.17}$$

One can check that the integrand in Eq. (B.17) can be expressed as a Laplace operator acting on a scalar function w_1, as follows:

$$\left(\frac{1}{\rho_A^3}+\frac{1}{\rho_B^3}\right)^2 w = \nabla^2 w_1, \tag{B.18}$$

$$
\begin{aligned}
w_1 \equiv{}& \frac{3}{2L^9}\ln^2\left(\frac{\rho_A}{\rho_B}\right)\\
&+\left[\frac{1}{8}\left(\frac{\rho_A^4}{\rho_B^4}-\frac{\rho_B^4}{\rho_A^4}\right)+\left(\frac{\rho_A^2}{\rho_B^2}-\frac{\rho_B^2}{\rho_A^2}\right)\left(\frac{L^4}{8\rho_A^2\rho_B^2}-1\right)-\left(\frac{\rho_A}{\rho_B}-\frac{\rho_B}{\rho_A}\right)^3\frac{L^2}{4\rho_A\rho_B}\right]\frac{1}{L^9}\\
&\times\ln\left(\frac{\rho_A}{\rho_B}\right)+\left(\frac{\eta_6}{480}+\frac{167\eta_4}{13440}-\frac{\eta_3}{84}-\frac{1}{192}\right)\frac{1}{L\rho_A^4\rho_B^4}\\
&+\left(-\frac{\eta_7}{192}-\frac{121\eta_5}{2688}+\frac{\eta_4}{28}-\frac{1061\eta_3}{13440}+\frac{13\eta_2}{420}+\frac{\eta_1}{16}\right)\frac{1}{L^3\rho_A^3\rho_B^3}\\
&+\left(\frac{\eta_8}{192}+\frac{57\eta_6}{896}-\frac{\eta_5}{42}+\frac{1289\eta_4}{6720}-\frac{113\eta_3}{105}-\frac{3271\eta_2}{13440}-\frac{19\eta_1}{70}+\frac{65}{24}\right)\frac{1}{L^5\rho_A^2\rho_B^2}\\
&+\left(-\frac{\eta_9}{384}-\frac{107\eta_7}{2688}-\frac{251\eta_5}{1680}+\frac{76\eta_4}{35}+\frac{107\eta_3}{168}+\frac{24\eta_2}{7}+\frac{5401\eta_1}{960}-\frac{88}{150}\right)\frac{1}{L^7\rho_A\rho_B}\\
&+\left(\frac{\eta_{10}}{1920}+\frac{25\eta_8}{2688}+\frac{491\eta_6}{13440}-\frac{152\eta_5}{175}-\frac{713\eta_4}{1680}-\frac{88\eta_3}{105}+\frac{15149\eta_2}{2240}+\frac{128\eta_1}{15}\right)\frac{1}{L^9},
\end{aligned}
\tag{B.19}
$$

where η_k is defined by the expression

$$\eta_k \equiv \left(\frac{\rho_A}{\rho_B}\right)^k+\left(\frac{\rho_B}{\rho_A}\right)^k (k=1,2,\ldots).$$

Substituting Eq. (B.18) into Eq. (B.17) and applying the divergence theorem, we get:

$$I_2=-\frac{3r_c^9}{32\pi}\int_{-\infty}^{\infty}\frac{\partial w_1}{\partial x}|_{x=0}\,dy-\frac{3r_c^{10}}{32\pi}\int_0^{2\pi}\frac{\partial w_1}{\partial \rho_B}|_{\rho_B=r_c}\,d\phi_B. \tag{B.20}$$

The symmetry of the function $w_1(x,y)$ implies that the integral along the y-axis is zero, and then Eq. (B.20) reduces to:

$$I_2=-\frac{3r_c^{10}}{32\pi}\int_0^{2\pi}\cdot\left.\frac{\partial w_1}{\partial \rho_B}\right|_{\rho_B=r_c}d\phi_B. \tag{B.21}$$

Substituting w_1 from Eq. (B.19) in Eq. (B.21) and expanding the obtained result in series for small $\lambda\equiv r_c/L$, we obtain:

$$I_2=\frac{63\lambda^4}{320}+\frac{\lambda^5}{256}+\frac{435}{512}\lambda^6+\frac{153}{128}\lambda^7+\frac{2753}{4096}\lambda^8+o(\lambda^8). \tag{B.22}$$

Finally, substituting Eqs. (B.15) and (B.22) into Eq. (B.10) we derive Eq. (4.5), which expresses the force coefficient $f_x^{(p)}$.

References

[1] M.G. Nikolaides, A.R. Bausch, M.F. Hsu, A.D. Dinsmore, M.P. Brenner, C. Gay, D.A. Weitz, Nature 420 (2002) 299–301.
[2] P.A. Kralchevsky, V.N. Paunov, I.B. Ivanov, K. Nagayama, J. Colloid Interface Sci. 151 (1992) 79–94.
[3] N.D. Denkov, O.D. Velev, P.A. Kralchevsky, I.B. Ivanov, H. Yoshimura, K. Nagayama, Langmuir 8 (1992) 3183–3190.
[4] V.N. Paunov, P.A. Kralchevsky, N.D. Denkov, K. Nagayama, J. Colloid Interface Sci. 157 (1993) 100–112.
[5] M. Yamaki, J. Higo, K. Nagayama, Langmuir 11 (1995) 2975–2978.
[6] D. Stamou, C. Duschl, D. Johannsmann, Phys. Rev. E 62 (2000) 5263–5272.
[7] P.A. Kralchevsky, N.D. Denkov, K.D. Danov, Langmuir 17 (2001) 7694–7705.
[8] N.D. Vassileva, D. van den Ende, F. Mugele, J. Mellema, Langmuir 21 (2005) 11190–11200.
[9] T.S. Horozov, B.P. Binks, Colloids Surf. A 267 (2005) 64–73.
[10] T.S. Horozov, R. Aveyard, B.P. Binks, J.H. Clint, Langmuir 21 (2005) 7405–7412.
[11] M.A. Ray, J. Li, Adv. Mater. 19 (2007) 2020–2022.
[12] E.P. Lewandowski, J.A. Bernate, P.C. Searson, K.J. Stebe, Langmuir 24 (2008) 9302–9307.
[13] R. di Leonardo, F. Saglimbeni, G. Ruocco, Phys. Rev. Lett. 100 (2008) 106103.
[14] J.C. Loudet, B. Pouligny, Europhys. Lett. 85 (2009) 28003.
[15] P.A. Kralchevsky, K. Nagayama, Langmuir 10 (1994) 23–36.
[16] P.A. Kralchevsky, K. Nagayama, Adv. Colloid Interface Sci. 85 (2000) 145–192.
[17] P.A. Kralchevsky, N.D. Denkov, Curr. Opin. Colloid Interface Sci. 6 (2001) 383–401.
[18] P.A. Kralchevsky, K. Nagayama, Particles at Fluid Interfaces and Membranes, Elsevier, Amsterdam, 2001.
[19] B.P. Binks, T.S. Horozov (Eds.), Colloidal Particles at Liquid Interfaces, Cambridge University Press, Cambridge, UK, 2006.
[20] C. Zeng, H. Bissig, A.D. Dinsmore, Solid State Commun. 139 (2006) 547–556.
[21] T.N. Hunter, R.J. Pugh, G.V. Franks, G.J. Jameson, Adv. Colloid Interface Sci. 137 (2008) 57–81.
[22] M. Oettel, S. Dietrich, Langmuir 24 (2008) 1425–1441.
[23] P.A. Kralchevsky, K.D. Danov, in: V.M. Starov (Ed.), Nanoscience: Colloidal and Interfacial Aspects, CRC Press, Boca Raton, FL, 2010 (Chapter 15).
[24] M. Megens, J. Aizenberg, Nature 424 (2003) 1014.
[25] K.D. Danov, P.A. Kralchevsky, M.P. Boneva, Langmuir 20 (2004) 6139–6151.
[26] K.D. Danov, P.A. Kralchevsky, J. Colloid Interface Sci. 298 (2006) 213–231.
[27] K.D. Danov, P.A. Kralchevsky, M.P. Boneva, Langmuir 22 (2006) 2653–2667.
[28] L. Foret, A. Würger, Phys. Rev. Lett. 92 (2004) 058302.
[29] A. Würger, L. Foret, J. Phys. Chem. B 109 (2005) 16435–16438.
[30] M. Oettel, A. Domínguez, S. Dietrich, Phys. Rev. E 71 (2005) 051401.
[31] M. Oettel, A. Domínguez, S. Dietrich, J. Phys: Condensed Matter 17 (2005) L337–L342.
[32] A. Domínguez, M. Oettel, S. Dietrich, J. Chem. Phys. 127 (2007) 204706.
[33] B.J. Park, J.P. Pantina, E.M. Furst, M. Oettel, S. Reynaert, J. Vermant, Langmuir 24 (2008) 1686–1694.
[34] M.P. Boneva, N.C. Christov, K.D. Danov, P.A. Kralchevsky, Phys. Chem. Chem. Phys. 9 (2007) 6371–6384.
[35] M.P. Boneva, K.D. Danov, N.C. Christov, P.A. Kralchevsky, Langmuir 25 (2009) 9129–9139.
[36] P. Pieranski, Phys. Rev. Lett. 45 (1980) 569–572.
[37] A.J. Hurd, J. Phys. A: Math. Gen. 18 (1985) L1055–L1060.
[38] V.N. Paunov, Colloid Polym. Sci. 281 (2003) 701–707.
[39] R. Aveyard, J.H. Clint, D. Nees, V.N. Paunov, Langmuir 16 (2000) 1969–1979.
[40] R. Aveyard, B.P. Binks, J.H. Clint, P.D.I. Fletcher, T.S. Horozov, B. Neumann, V.N. Paunov, J. Annesley, S.W. Botchway, D. Nees, A.W. Parker, A.D. Ward, A.N. Burgess, Phys. Rev. Lett. 88 (2002) 246102.
[41] T.S. Horozov, R. Aveyard, J.H. Clint, B.P. Binks, Langmuir 19 (2003) 2822–2829.
[42] M.E. Leunissen, A. van Blaaderen, A.D. Hollingsworth, M.T. Sullivan, P.M. Chaikin, Proc. Natl. Acad. Sci. 104 (2007) 2585–2590.
[43] M.E. Leunissen, J. Zwanikken, R. van Roij, P.M. Chaikin, A. van Blaaderen, Phys. Chem. Chem. Phys. 9 (2007) 6405–6414.
[44] S. Wu, A. Nikolov, D. Wasan, Can. J. Chem. Eng. 85 (2007) 562–569.
[45] L.D. Landau, E.M. Lifshitz, Electrodynamics of Continuous Media, Course of Theoretical Physics, vol. 8, Pergamon Press, Oxford, 1960.
[46] L.E. Scriven, Chem. Eng. Sci. 12 (1960) 98–108.
[47] P.A. Kralchevsky, V.N. Paunov, N.D. Denkov, I.B. Ivanov, K. Nagayama, J. Colloid Interface Sci. 155 (1993) 420–437.
[48] J.D. Jackson, Classical Electrodynamics, Wiley, New York, 1962.
[49] K.D. Danov, P.A. Kralchevsky, K.P. Ananthapadmanabhan, A. Lips, Langmuir 22 (2006) 106–115.
[50] A.P. Philipse, A. Vrij, J. Colloid Interface Sci. 128 (1989) 121–136.
[51] K.D. Danov, P.A. Kralchevsky, B.N. Naydenov, G. Brenn, J. Colloid Interface Sci. 287 (2005) 121–134.
[52] I.E. Tamm, Fundamentals of the Theory of Electricity, Mir Publishers, Moscow, 1979.
[53] K.D. Danov, P.A. Kralchevsky, Adv. Colloid Interface Sci. (2010). doi:10.1016/j.cis.2010.01.01.